Materials and Design 160 (2018) 794–802

Contents lists available at ScienceDirect

Materials and Design

journal homepage: www.elsevier.com/locate/matdes

Novel method of phosphorescent strontium aluminate coating preparation on aluminum

Ivita Bite, Guna Krieke, Aleksejs Zolotarjovs, Katrina Laganovska, Virginija Liepina, Krisjanis Smits *, Krisjanis Auzins, Larisa Grigorjeva, Donats Millers, Linards Skuja

Institute of Solid State Physics, University of Latvia, Latvia

HIGHLIGHTS

- A new one-step plasma electrolytic oxidation process of strontium aluminate coating on aluminum alloy is demonstrated.
- It was applied for production of an efficient long-afterglow phosphor $SrAl_2O_4$: Eu^{2+},Dy^{3+} on aluminium alloy Al6082.
- The obtained coating exhibits optical properties similar to commercial $SrAl_2O_4$: Eu^{2+}, Dy^{3+} phosphor.
- The formation of strontium aluminate occurs during the local high-temperature plasma discharges.
- This method provides an engineering solution for metal surface coatings having *both* protective and functional properties.

GRAPHICAL ABSTRACT

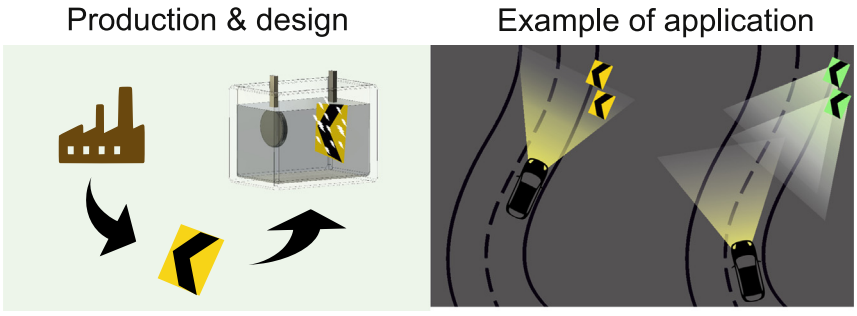

ARTICLE INFO

Article history:
Received 12 July 2018
Received in revised form 12 October 2018
Accepted 13 October 2018
Available online 15 October 2018

Keywords:
Phosphorescent coating
Strontium aluminate
Long afterglow
Persistent luminophore
Electrolytic oxidation

ABSTRACT

This study presents a novel approach to produce phosphorescent coatings on metal surfaces.
Strontium aluminates are the most popular modern phosphorescent materials exhibiting long afterglow at room temperature and a broad spectral distribution of luminescence in the visible range. However, despite a large amount of research done, methods for synthesis of such materials remain relatively energy inefficient and environmentally unfriendly.
A long-afterglow luminescent coating containing $SrAl_2O_4$:Eu^{2+}, Dy^{3+} is prepared by the plasma electrolytic oxidation on the surface of commercial aluminum alloy Al6082. During the electrical discharges in this process, the strontium aluminate is formed in a similar way to the solid-state reaction method. X-ray powder diffraction analysis confirms that the monoclinic $SrAl_2O_4$ phase is present in the coating.
Optical properties of the obtained coating were analyzed with luminescence methods classically used for studies of luminophores. The performance of the coating was compared with commercially available strontium aluminate powder.
The proposed method of coating synthesis may be of value for the development of energy-efficient and long-lasting automotive and public safety infrastructure.

© 2018 Elsevier Ltd. This is an open access article under the CC BY-NC-ND license (http://creativecommons.org/licenses/by-nc-nd/4.0/).

1. Introduction

The present research is devoted to the development of a new application for metal protective coatings. The aim is to produce mechanically and chemically stable coating with added luminescent properties

* Corresponding author.
E-mail address: smits@cfi.lu.lv (K. Smits).

https://doi.org/10.1016/j.matdes.2018.10.021
0264-1275/© 2018 Elsevier Ltd. This is an open access article under the CC BY-NC-ND license (http://creativecommons.org/licenses/by-nc-nd/4.0/).

obtained by the synthesis of long-lasting luminescence materials such as the most popular phosphor SrAl.

Since the discovery of long-lasting luminescence of rare earth (RE) doped strontium aluminates (SrAl) in 1996 by Matsuzawa [1], SrAl phosphors doped with divalent europium and trivalent dysprosium ions ($SrAl_2O_4$:Eu^{2+}, Dy^{3+}) have been extensively studied [2–9]. This phosphor material group was proven to be superior to others in many ways. SrAl doped by RE shows excellent luminescence properties such as green phosphorescence with long lifetime (>10 h [10–13]) and high quantum efficiency [2,3,14], good thermal and chemical stability [5,15], environmental friendliness and nontoxicity [5,16,17]. For these reasons, SrAl is already used in a wide range of industrial applications such as traffic and emergency signs [5,18], white-light emitting diodes [6,16], textile printing [5], biological markers [2,16], as luminous paints in airports, highways and buildings [3,19] etc.

Strontium aluminates glow in the blue-green region of the spectrum – the maximum of the emission shifts depending on the host matrix including different compositions of SrAl, therefore the emission color is tunable [20]. The luminescence center in these materials is Eu^{2+}, responsible for broad emission band. Dy^{3+} co-activation enhances the luminescent properties of the phosphor, making the afterglow brighter and longer. The work on prolonging the afterglow of strontium aluminates is still ongoing [20], focusing on altering the defects in the material, therefore raising hope that the duration of afterglow in SrAl will become even longer. The excellent spectroscopic properties of these hosts make them attractive for various practical applications in different forms, including coatings.

Long-afterglow luminescent materials presently are used mostly in the form of luminescent paint. The luminescent signs, labels as well as road schemes are typically fabricated via injecting long-afterglow material in a paint layer. This method has multiple drawbacks: low efficiency, weak adhesion, complicated preparation process etc. Therefore, new ways of obtaining SrAl should be developed. One of the emerging methods is Plasma Electrolytic Oxidation (PEO) process, well-known for the production of ceramic coatings, however, up to now rarely used to obtain luminescent coatings.

PEO is a technology for producing hard ceramic coatings on various valve metal surfaces. Developed in the 70s [21], this method is often called micro-arc oxidation (MAO) [22] or plasma electrolytic deposition (PED). The technology is based on anodization with the main difference being the use of a higher voltage/current to achieve plasma discharges through the dielectric layer of the freshly formed oxide coating. PEO process allows the creation of ceramic and crystalline structures due to the high temperature (up to several thousands of degrees [23]) and pressure in highly localized plasma discharges. Many researchers also point out the possibility to obtain the hardest alumina phase – corundum (hexagonal, α-phase) [24–26]. Hardness [27,28] combined with excellent chemical stability [26,28–30] of the coatings shows great potential for use in many practical applications where high-quality protective layers are required. In addition, it was demonstrated that the composition of the coating can be modified by particle addition in the electrolyte [31] which opens great possibilities for development of functionalized PEO coatings. Obtaining luminescent coatings via PEO process at presents opens a new field of opportunity for practical applications. During the recent years, the combination of outstanding mechanical properties with functionalization of the PEO coatings has attracted a growing attention. Intense studies of modification of PEO coatings were carried out to obtain efficient luminescence output used for acquiring the information about the quality of the coating [32] as well as for sensor development. An example of a possible new application is the ZnO PEO coating – it was demonstrated that the luminescence response shows sensitivity to the oxygen content in the surrounding gasses [33]. Since RE ions are well-known as efficient luminescence centers in many matrices, an essential direction of research is the process of incorporation of RE ions in PEO coatings. Three main approaches were developed and successfully applied to embed RE ions in the structure of the coating and to observe the luminescence output: alloy doping [32], electrolyte doping and pore filling technique [34,35].

Since this study is aimed at the possible industrial applications, one of the most common aluminum alloys Al6082 is used as a substrate for the coatings. In addition, the industry-friendly one-step process of doping (using modified electrolyte) was used to obtain RE doped SrAl coating. To the authors' best knowledge, this is the first time SrAl PEO coating is obtained and also the first time the long-lasting luminescence is observed from a PEO coating. The addition of long-lasting luminescence to PEO coatings can create new applications in various fields.

2. Experimental section

The preparation and characterization of the physical properties of long afterglow luminescent PEO coating are shown schematically in Fig. 1.

2.1. Materials and sample preparation

Strontium carbonate ($SrCO_3$, purity 99.99%), europium oxide (Eu_2O_3, purity 99.99%), dysprosium oxide (Dy_2O_3, purity 99.9%) were used as the starting materials and were purchased from Alfa Aesar. Analytical grade chemicals were used without any further purification. The electrolyte solutions were prepared with deionized water and

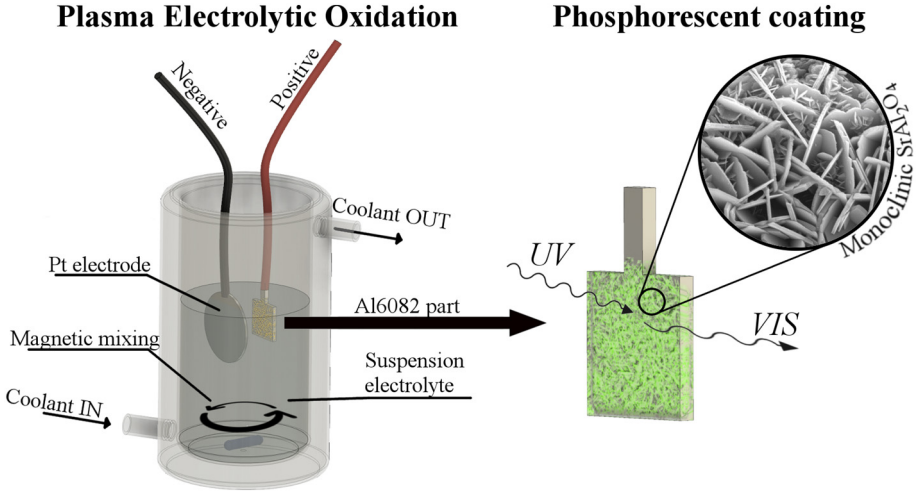

Fig. 1. Graphical representation of preparation and characterization of the physical properties of the long afterglow luminescent PEO coating.

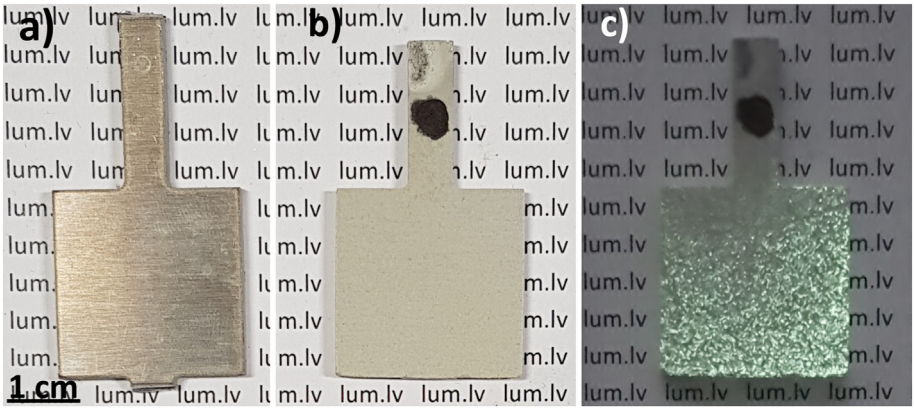

Fig. 2. The surface of Al6082 before (a) and after the PEO process (b), as well as observed green afterglow luminescence from the PEO coating after UV irradiation (c).

potassium hydroxide (KOH, STANLAB). The deionized water with the conductivity of <0.1 μS cm^{-1} was obtained from ADRONA Crystal 7 Pure water purification system.

Commercial SrAl powder ($Sr_{0,95}Eu_{0,02}Dy_{0,03}Al_2O_4$, purity ≥ 99%) was purchased from Sigma Aldrich and was used as a reference material for the long afterglow luminescence comparison purposes.

Commercial aluminum alloy (Al6082) was used as one of the working electrodes in experiments. Al6082 samples were cut by water jet from 3 mm thick non-polished Al6082 plate, the final size of Al6082 samples was 25 × 25 × 3 mm, yielding the total area of all 6 faces as 15.5 cm^2.

2.2. PEO coating preparation

Before the PEO process, Al6082 sample surface was cleaned with acetone, washed with deionized water and dried in air at room temperature. To produce long afterglow luminescent coatings, 5 kW bipolar pulse electric generator (A5V750/300) was used. Pt counter-electrode with a total surface area of 2.8 cm^2 was placed 3 cm from the Al6082 sample. A solution of 1 g L^{-1} KOH was used as a base for electrolyte with pH of 12.4; 6.0 g of $SrCO_3$, 0.5 g of Eu_2O_3 and 1.0 g of Dy_2O_3 was added to obtain a white suspension. The electrolyte was placed in a double-walled tempered glass reactor with an active water cooling system. A constant voltage-limited (with voltage 700 V and a current density around 0.18 A cm^{-2}) unipolar regime was applied. Anodization stage was observed with no plasma discharges for the first 150 s of the process, followed by a homogeneous distribution of plasma arcs on the surface of the sample for the remaining process time. The PEO coating of average thickness 40 μm was formed in one-hour time. A slight decrease of the current draw was observed with the current reduced from 0.19 A cm^{-2} to 0.17 A cm^{-2} in the last 15 min of the process. The decrease is mostly due to the increase in thickness of the oxide layer as well as the loss of electrolyte by evaporation. After the PEO process, the sample was washed with an HCl solution to remove the excess of $SrCO_3$ from the PEO coating surface, then rinsed with deionized water and dried at room temperature in air.

2.3. Characterization techniques

The crystalline phases of the long afterglow luminescent PEO coating were characterized by X-ray powder diffraction (XRD, PANalytical X'Pert Pro diffractometer) using a cathode voltage of 45 kV and current of 40 mA with Cu K_α radiation (1.5418 Å). The morphology and chemical composition of the long afterglow luminescent PEO coating were characterized by scanning electron microscopy (SEM, Tescan Lyra) equipped with energy dispersive X-ray spectrometer (EDX) operated at 15 kV. Prior to examination, the sample was coated with a gold layer. The morphology and additional element distribution studies were performed using a transmission electron microscope (TEM, Tecnai G2 F20, FEI) operated at 200 kV. The samples for TEM studies were scratched from coating using diamond pen and placed on a lacy carbon coated grid AGS166-4 (Agar Scientific).

The luminescence was studied using two excitation sources: the deuterium lamp through Jobin Yvon TRIAX320 excitation monochromator for excitation spectrum recording as well as for afterglow and kinetics measurements; and X-ray tube (W target, 30 kV, 10 mA) for

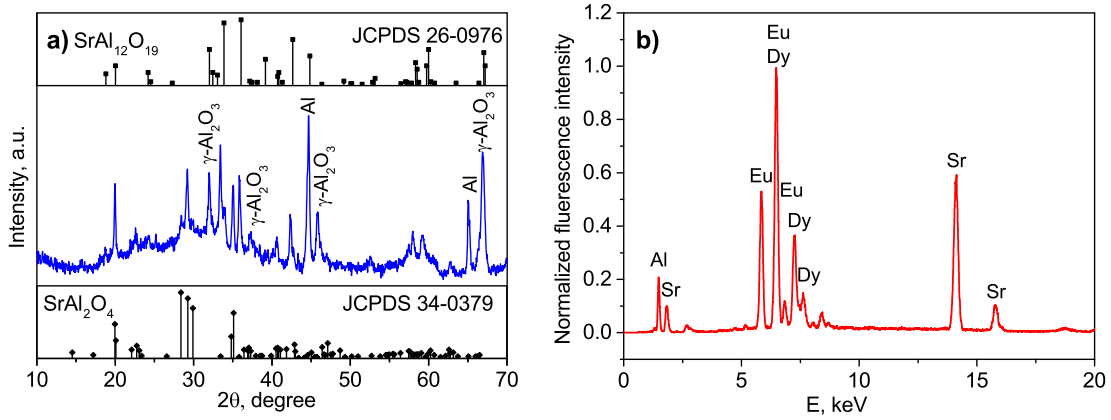

Fig. 3. a) XRD pattern and b) EDX spectrum of PEO coated Al6082 surface.

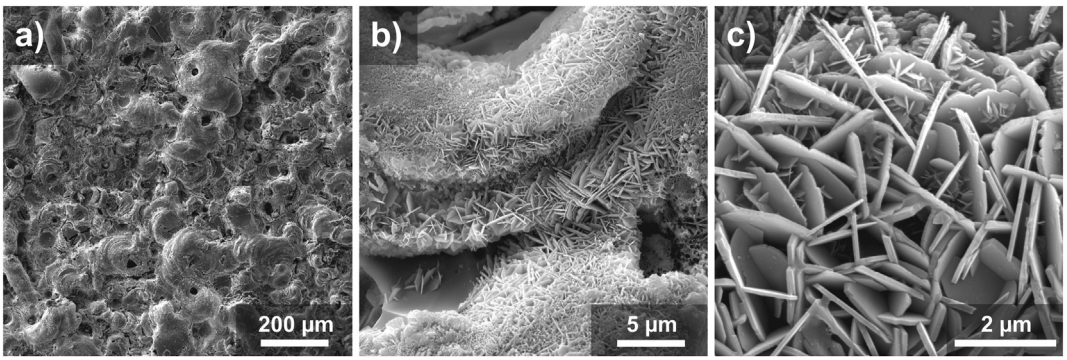

Fig. 4. SEM micrographs of PEO coated Al6082 surface.

excitation of thermostimulated luminescence (TSL). The detection was performed using two systems: the Andor Shamrock B-303i spectrograph coupled with Andor DU-401A-BV CCD camera was used for TSL measurements; Horiba SR330 monochromator equipped with 150 l/mm diffraction grating coupled with Hamamatsu R928P PMT tube was used to register excitation spectrum, photoluminescence and kinetics. The TSL was recorded using a custom-built heating system to linearly heat the sample with the speed of 2 K s^{-1}.

3. Results and discussion

3.1. Phase composition and morphology of PEO coating

Starting with an unpolished metallic sample of Al6082 alloy, a matte grey oxide coating was grown on the surface (see Fig. 2a and b). The coating exhibits green luminescence afterglow after a short irradiation with ultraviolet (UV) light (390 nm, FWHM 20 nm) (Fig. 2c). One can observe that the glow of the coating is uneven. The luminescent dot size is similar to plasma discharge channel, therefore one can conclude that the emission is observed near them.

XRD pattern of the long afterglow luminescent PEO coating is shown in Fig. 3a. Several peaks corresponding to γ-Al_2O_3 and Al from the substrate can be observed. In addition, XRD peaks that agree well with the most intensive peaks of monoclinic $SrAl_2O_4$ can also be detected. The relative intensity of the peaks differs from the reference sample, possibly indicating anisotropic growth of $SrAl_2O_4$. The XRD pattern suggests that another aluminate phase – hexagonal $SrAl_{12}O_{19}$ might also be present in the coating. No crystalline phases containing the dopant ions (Dy^{3+} and Eu^{2+}/Eu^{3+}) could be detected; therefore, we can expect the incorporation of these ions in the crystalline lattices of strontium aluminates or alumina. The EDX spectrum of PEO-coated Al6082 surface is shown in Fig. 3b. The presence of Sr, Eu and Dy in the coating is detected confirming the incorporation of both rare earth and strontium ions in the coating. The EDX analysis revealed the approximate ratio of elements to be 67% Al, 22% Sr, 4% Eu, 7% Dy at.%, which is in good agreement with the intended composition of $SrAl_2O_4$:Eu^{2+}, Dy^{3+}.

Fig. 4 shows the morphology of the surface of the coating. At lower magnifications, microstructures typical to PEO coating can be observed - with characteristic pores and microcracks (see Fig. 4a). At higher resolution, the formation of platy microcrystals is observed (see Fig. 4b and c). The crystals are assumed to be strontium aluminates with the average length of 1–5 μm and thickness ranging from 100 to 150 nm. The platy morphology of crystals is often desirable and is proven to enhance ferroelectric and electromagnetic properties [36–40]. EDX results confirm that all elements from the insoluble additives (Sr, Eu and Dy) of the electrolyte are present in PEO coating.

The cross-section of the obtained coating was inspected using SEM (Fig. 5). The average thickness of the coating was estimated to be approximately 40 μm. EDX map of element distribution was measured in SEM (Fig. 6). In addition to the aluminum, strontium and oxygen, rare earth elements are distributed evenly in the coating (although Dy and Eu signals are close to the detection limit of the setup – their concentration in the coating is low).

The morphology and chemical composition homogeneity of the crystals observed in the PEO coating were characterized using high resolution TEM. The bright field TEM image of an individual platy particle is shown in Fig. 7a. The dark field TEM images at different rotation angles (see Fig. 7b–e) revealed the presence of nanocrystals with different crystallographic orientations showing the polycrystalline nature of the platy particles and the "tree" type crystal structure is possibly related to ion diffusion channels during electrical discharges.

Typical element distribution maps of the same particle are shown in Fig. 7f–j. Intense signal from Sr, Al, O, Eu and Dy was detected, indicating the formation of rare earth doped strontium aluminate. Signal from Eu and Dy atoms is detected in all of the platy type particle, confirming the incorporation of the rare earth activators in the crystalline phase. In addition, some regions enriched predominantly by Al and O can be observed, (left upper corner in Fig. 7g–h) supporting XRD data which indicate the presence of Al_2O_3 in the PEO coating as well small particles with higher Sr concentration (Fig. 7f) and Dy concentration (Fig. 7j). This rises suggestion that these small particles are not melted together and thus the element distribution homogeneity is low.

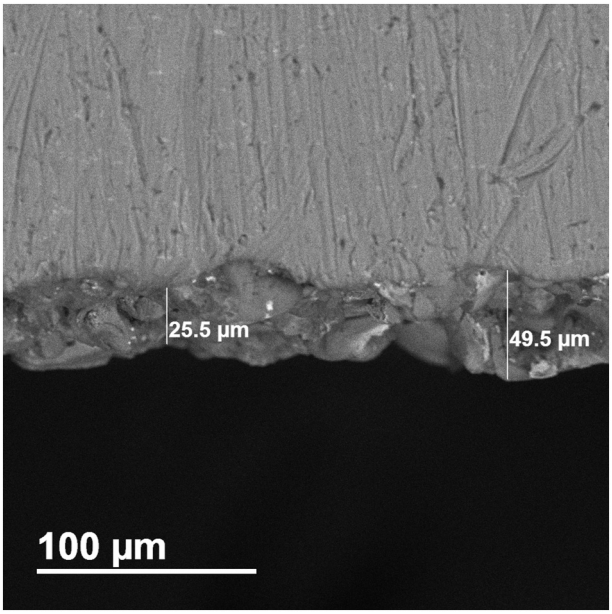

Fig. 5. SEM BSE image of the cross-section of PEO coated Al6082 surface.

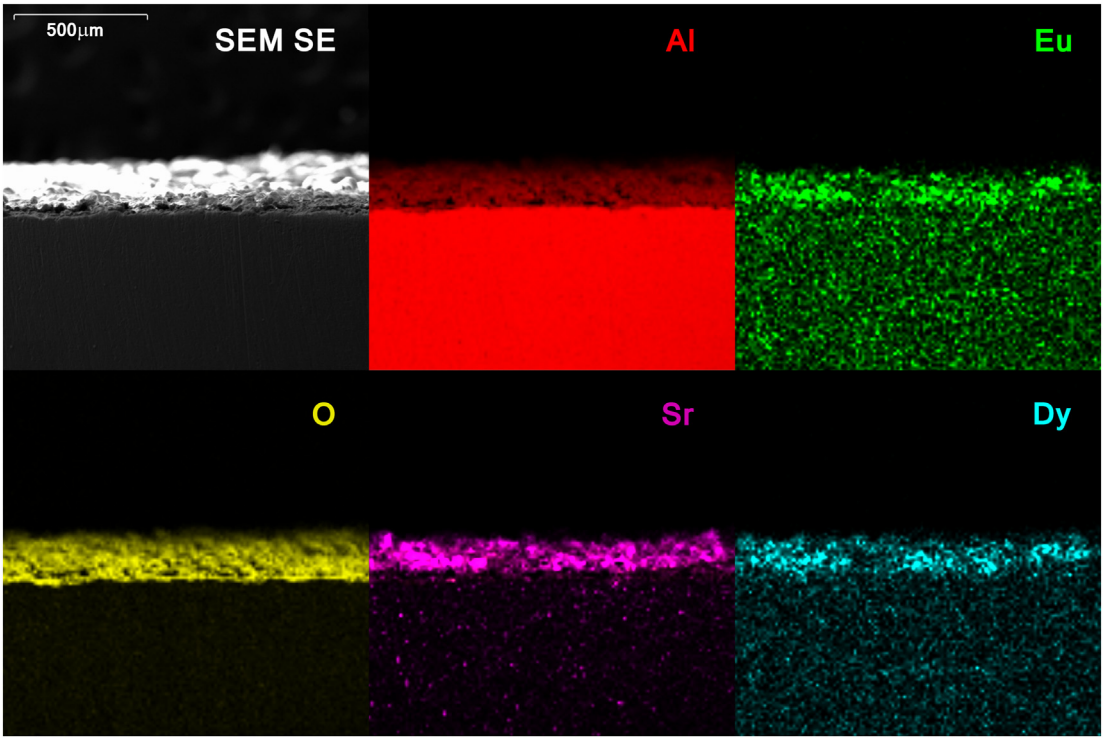

Fig. 6. SEM EDX mapping of PEO coated Al6082 surface.

3.2. Luminescence measurements

The luminescence properties of the obtained coating were compared to those of a commercially available SrAl (Sigma Aldrich), used as a reference. Luminescence excitation, emission and afterglow were measured at room temperature. The spectral distributions of afterglow (long-lasting luminescence, phosphorescence) from the obtained coating and commercial SrAl are almost identical indicating that the afterglow luminescence centers of both coating and commercial powder are the same (Fig. 8b). However, an additional peak appears under UV (320 nm) excitation at 455 nm (2.72 eV) in the emission spectrum of the coating.

The 520 nm peak can be attributed to the typical 5d-4f emission of Eu^{2+} [41]. This peak is present in the emission spectra of both samples and is the evidence of Eu^{2+} ion incorporation in the PEO layer. The luminescence band at 520 nm is strong evidence that during the formation of PEO coating $SrAl_2O_4$ containing Eu^{2+} is created, thus the Eu^{3+} is reduced.

The second maximum at 455 nm (2.72 eV), present only in PL of the coating could be associated with Eu^{2+} ion incorporation in another Sr position of the SrAl matrix [42]; however, some contribution from the intrinsic amorphous alumina luminescence [43,44] cannot be excluded. It is noted in literature that this maximum is thermally quenched at temperatures starting from 150 K [2,45]; therefore, it might also be

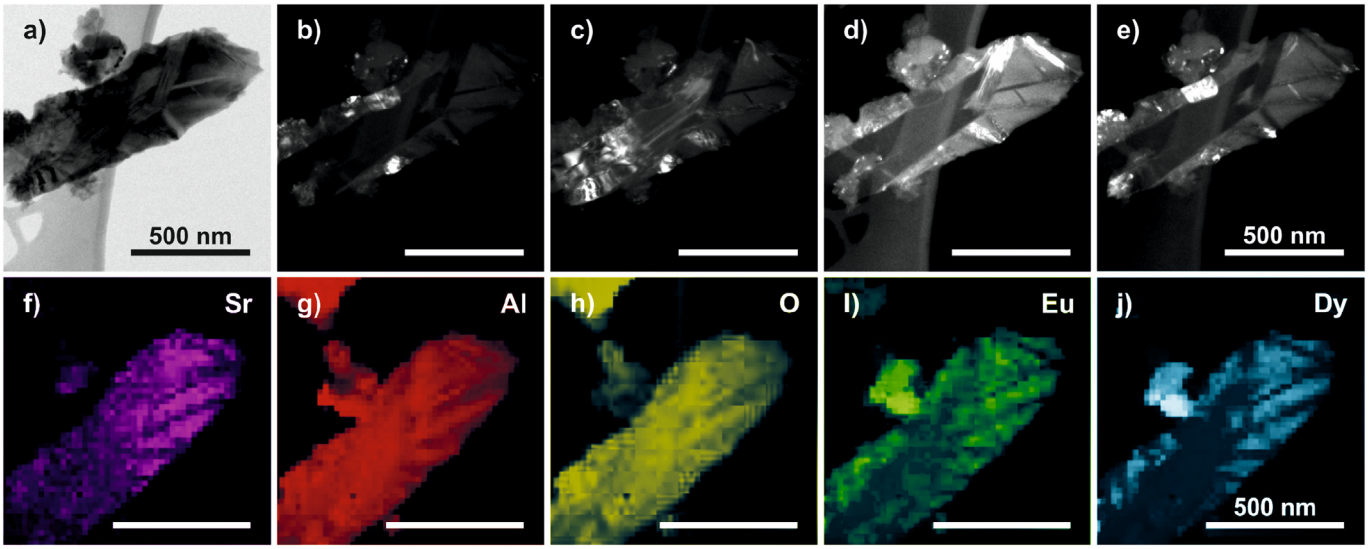

Fig. 7. TEM micrographs of an individual platy particle isolated from PEO coating: a) bright field, b–e) dark field, f–j) element mapping images.

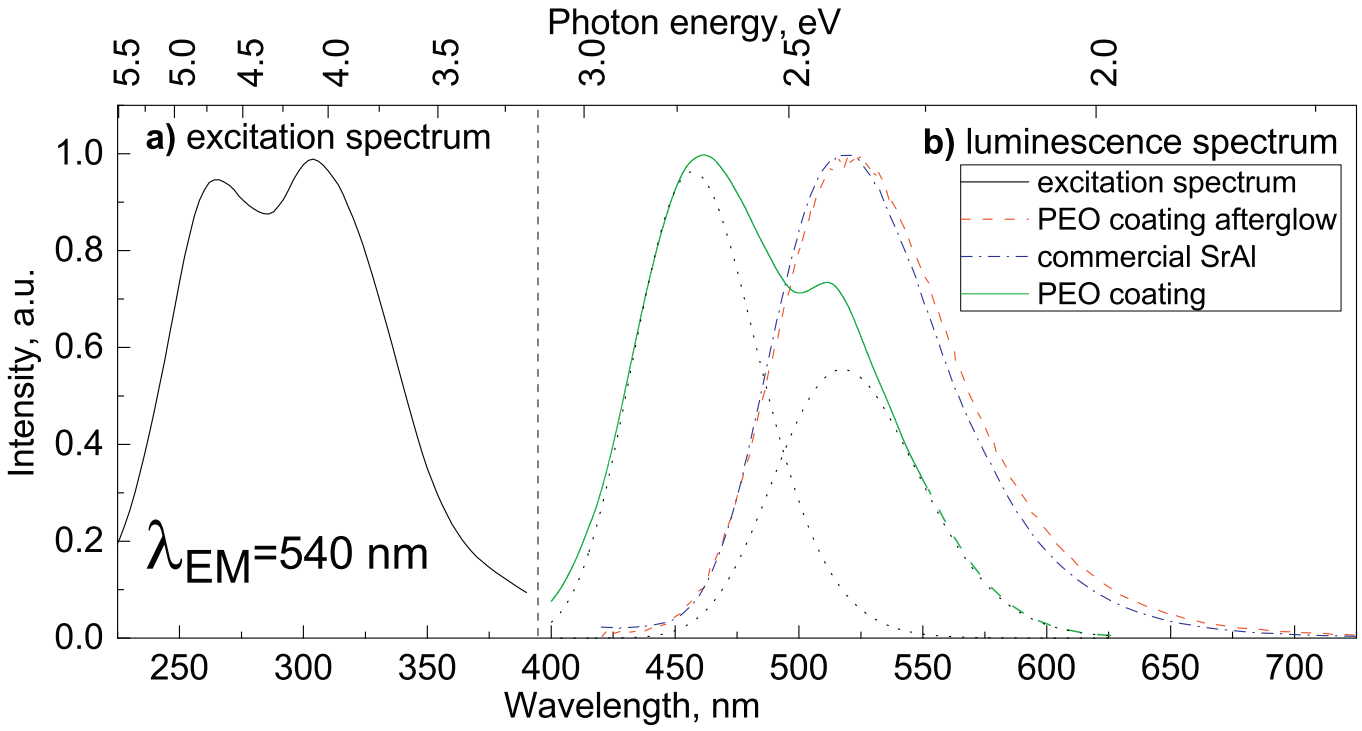

Fig. 8. a) Excitation spectrum of the coating measured at 540 nm b) Luminescence spectra of the coating under UV irradiation at 320 nm (solid line, dotted lines show Gaussian components), the afterglow from the coating (dashed line) as well as the afterglow of the reference SrAl sample (dash-dotted line).

attributed to the luminescence emerging from different strontium aluminate compounds present in the coating. Dutczak et al. [20] have concluded that the changes in Sr/Al ratio strongly affect the position of the 4f6-5d1-4f7 emission of Eu^{2+}. We noted beforehand that XRD measurements show some traces of different aluminate that might be present in the coating. The research paper [20] shows different positions of maxima depending on the host and 455 nm maximum might be attributed to $SrAl_4O_7$:Eu luminescence.

To determine if there is any alumina intrinsic defect luminescence contribution, undoped alumina coating is prepared and studied. The 455 and 520 nm luminescence bands were not observed in the luminescence spectrum of the undoped coating. This observation draws a logical conclusion that the band at 455 nm indeed somehow relates to Eu^{2+} emission in the SrAl matrix and cannot be associated with alumina intrinsic defects luminescence [46–48]. This conclusion correlates well with the general observation of Eu^{2+} ion in various other aluminate matrices (BaMgAl, BaEuAl etc.) [8,49].

The excitation spectrum measured for the 520 nm emission band (Fig. 8a) consists of two peaks. The overall shape and position of the excitation spectrum are similar to those of SrAl reported in other studies [50].

The physical phenomenon behind long-lasting luminescence in SrAl is thermally assisted charge release from electron traps, followed by the electron recombination at luminescence center. Therefore, it is crucial to perform thermostimulated luminescence (TSL) measurement above the room temperature (Fig. 9). A broad, intense and possibly complex glow peak was observed. The maximum of glow peak is at 425 K, the FWHM is 144 K.

The spectrum of TSL is the same as recorded for afterglow and this is in accordance with the mechanism of long afterglow as discussed in [8,51]. The main idea of this mechanism is that electron is thermally released from some trap and recombines with Eu^{3+}. Thus, the excited Eu^{2+} center is created, and its radiative decay is the origin of the observed luminescence. Since the initial rise of glow curve is slightly above room temperature, the probability of electrons to be released from the trap is low, the process of emptying of the traps takes a long time and the afterglow can be observed. The actual TSL luminescence phenomena are usually much more complex than the “single trap” model, and the complex TSL glow curve of the studied coating confirms that.

Luminescence kinetic was measured at room temperature (Fig. 10) for the 520 nm band. The decay of the luminescence after short irradiation time ($t = 10$ s) can be best approximated with a stretched exponential function. The physical interpretation can be found in [52], stating a wide distribution of the energy levels (traps) that the electron can occupy around the charged ion (Eu^{2+} in our case). Disorder in oxide materials causes a distribution of trap energies and charge carrier release rates. This distribution is responsible for the multiple diffusion that arises from a multiple trapping–detrapping events. Therefore, the decay kinetics of luminescence is superposition from a number of exponential decays [53,54] and can be well approximated by the stretched

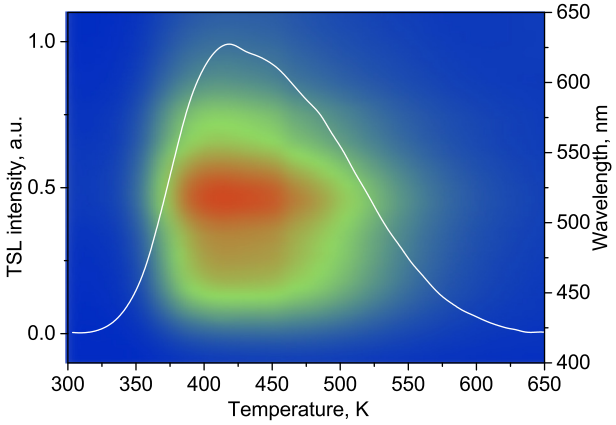

Fig. 9. Thermostimulated luminescence (TSL) measurement of the obtained coating.

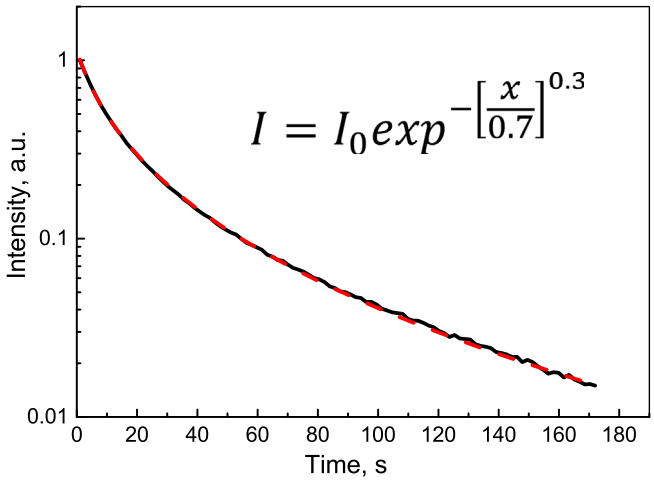

Fig. 10. Luminescence kinetic of the obtained coating at room temperature after 10 min of UV excitation. Red dashed line shows the stretched exponent approximation, the formula is inserted in the graph.

exponent. The stretch power 0.3 in our case is associated with the differences of trap energies. This statement correlates well with wide TSL glow curve maximum representing a wide range of trap energies.

A signal from strontium aluminate in aluminum PEO coating is detectable even min after the short irradiation with UV light; however, the sample still needs to be optimized for it to match the performance of commercially available SrAl powders (hours of afterglow). Using the PEO method for surface treatment, three different processes happen simultaneously – the electrochemical reactions, the plasma chemical reactions and thermal diffusion [55]. Electrochemical surface treatment using the PEO process on Al6082 is schematically illustrated in Fig. 11. During the PEO process a sufficient electric potential is applied, Al first reacts with basic electrolyte to form amorphous, nonconductive Al_2O_3 coating on the Al6082 surface by the following equation [56,57]:

$$2Al + 6OH^- \rightarrow Al_2O_3 + 3H_2O + 6e^- \quad (1)$$

At this stage, the voltage between Al6082 and the electrolyte is increasing until plasma discharges are created. These plasma discharges consequently cause a local plasma reaction that induces the high-temperature conditions which modify Al_2O_3 growth and initiates the reaction between Al_2O_3, $SrCO_3$, Eu_2O_3 and Dy_2O_3. Due to the high energy nature of the PEO process, the temperature of the plasma reaches 1400 °C [21] and according to the studies [58], hydrogen is formed in the plasmas discharge channels by exothermic reaction with water vapor. Thus, some elements change their charge states in the plasma discharges relative to those existing in the precursors. Thermal diffusion affects the oxygen (O^{2-}) migration from SrAl coating to the Al boundary surface thus forming Al_2O_3. The migration of oxygen increases the number of oxygen vacancies in the SrAl coating, therefore reducing Eu^{3+} to Eu^{2+}.

The formation of long afterglow luminescent coating, according to PEO method, can be described by the following equation:

$$Al_2O_3 + (1-x-y)SrCO_3 + xEu_2O_3 + yDy_2O_3 \rightarrow Sr_{1-x-y}Eu_xDy_yAl_2O_3 + (1-x-y)CO_2\uparrow \quad (2)$$

Similarly, the SrAl can be formed by the solid-state reaction method. The solid-state synthesis method of SrAl powder is described by the following equation [59–61]:

$$Al_2O_3 + 0.97SrCO_3 + 0.005Eu_2O_3 + 0.01Dy_2O_3 \xrightarrow[-H_2O;-N_xO_y;-CO_z]{1350^\circ C;H_2/N_2} Sr_{0.97}Eu_{0.01}Dy_{0.02}Al_2O_4 + 0.97CO_2\uparrow \quad (3)$$

Using the PEO method, the long afterglow luminescent coating can be prepared on the commercially available alloy Al6082 surface in one-step one-pot synthesis. In comparison with the most popular method of preparation of this material – solid-state reaction method, our approach provides various advantages. The most important one is the simplicity, especially when the luminescent coating is needed. In contrast, the powder formed by solid-state reaction still needs to be processed and deposited on the substrate. Another great advantage is the environmental friendliness of the PEO. When alternatively using the solid-state reaction method, a larger energy consumption is needed to anneal the powder at up to 1400 °C for several hours (2–4 h) [59–61] and reducing atmosphere ($N_2 + H_2$) is required in order to increase the number of oxygen vacancies and to reduce Eu^{3+} to Eu^{2+}. This leads to a pollution of the environment by NO_x and is a serious concern for volume production of the material.

4. Conclusions

For the first time, a long afterglow luminescent coating containing monoclinic $SrAl_2O_4$:Eu^{2+}, Dy^{3+} was produced on aluminum in the PEO process. To create it, $SrCO_3$, Eu_2O_3 and Dy_2O_3 powders were suspended in KOH based electrolyte and Al6082 aluminum alloy was used as a substrate. Excellent optical properties were observed: luminescence similar to that emitted by commercially available strontium aluminates, and a long afterglow after a short irradiation time. The luminescence band of Eu^{2+} observed in the spectrum of the long afterglow confirms that Eu^{3+} originating from Eu_2O_3 is reduced to Eu^{2+} in the process of PEO coating creation.

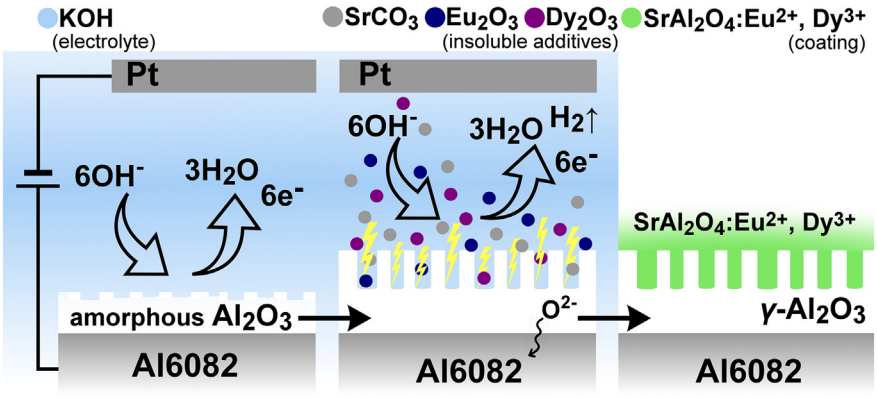

Fig. 11. Schematic illustration of the electrochemical process on the surface of Al6082 during the PEO treatment.

With the addition of novel luminescent properties, a completely new type of functional materials was obtained. The developed technology is offering a simple and cost-effective one step synthesis route for production of long afterglow luminescence coatings. It is promising for applications where both the metal protection from the environment (longevity) and the high visibility are desired. The simplest examples are the external parts of a car/plane or surface of the buildings/road signs and various types of emergency signs.

Author contribution

Ivita Bite together with Guna Krieke performed all chemistry operations (electrolyte content, analysis of the results, conclusions about the mechanism of RE ion incorporation in the coating) as well as XRD measurements.

Aleksejs Zolotarjovs with Katrina Laganovska performed all PEO synthesis.

Krisjanis Auzins performed PEO synthesis using different parameters.

Virginija Liepina with Katrina Laganovska performed the excitation and emission luminescence measurements, TSL study as well as helped with the analysis of the data.

Larisa Grigorjeva performed the kinetics measurement as well as helped with the interpretation of the results.

Krisjanis Smits performed SEM and EDX measurements and together with Aleksejs Zolotarjovs and Linards Skuja made the analysis of the results, final assembly of the paper as well as most result interpretation with the heavy help of Donats Millers with his decades of experience working with strontium aluminates.

Acknowledgments

This work was supported by the ERDF, European-Union Project No. 1.1.1.1/16/A/182.

References

[1] T. Matsuzawa, Y. Aoki, N. Takeuchi, Y. Murayama, A new long phosphorescent phosphor with high brightness, SrAl2O4:Eu2+,Dy3+, J. Electrochem. Soc. 143 (1996) 2670–2673.
[2] V. Liepina, D. Millers, K. Smits, Tunneling luminescence in long lasting afterglow of SrAl2O4:Eu,Dy, J. Lumin. 185 (2017) 151–154, https://doi.org/10.1016/j.jlumin.2017.01.011.
[3] Z. Xue, S. Deng, Y. Liu, B. Lei, Y. Xiao, M. Zheng, Synthesis and luminescence properties of SrAl2O4:Eu2+,Dy3+ hollow microspheres via a solvothermal co-precipitation method, J. Rare Earths 31 (2013) 241–246, https://doi.org/10.1016/S1002-0721(12)60265-8.
[4] V. Sharma, A. Das, V. Kumar, Eu $^{2+}$, Dy $^{3+}$ codoped SrAl $_2$ O $_4$ nanocrystalline phosphor for latent fingerprint detection in forensic applications, Mater. Res. Express 3 (2016), 15004. https://doi.org/10.1088/2053-1591/3/1/015004.
[5] D.P. Bisen, R. Sharma, Mechanoluminescence properties of SrAl $_2$ O $_4$:Eu $^{2+}$ phosphor by combustion synthesis, Luminescence 31 (2016) 394–400, https://doi.org/10.1002/bio.2972.
[6] H. Yamada, K. Nishikubo, C.N. Xu, Determination of Eu sites in highly europium-doped strontium aluminate phosphor using synchrotron X-ray powder diffraction analysis, J. Electrochem. Soc. 155 (2008) F139, https://doi.org/10.1149/1.2907407.
[7] D. Kim, H.E. Kim, C.H. Kim, Effect of composition and impurities on the phosphorescence of green-emitting alkaline earth aluminate phosphor, PLoS One 11 (2016) 1–12, https://doi.org/10.1371/journal.pone.0145434.
[8] K. Van den Eeckhout, P.F. Smet, D. Poelman, Persistent luminescence in Eu2+-doped compounds: a review, Materials (Basel) 3 (2010) 2536–2566, https://doi.org/10.3390/ma3042536.
[9] R.E. Rojas-Hernandez, F. Rubio-Marcos, M.V. Dos Santos Rezende, M.Á. Rodriguez, A. Serrano, Á. Muñoz-Noval, J.F. Fernandez, The impact of the synthesis conditions on SrAl2O4: Eu, Dy formation for a persistent afterglow, Mater. Des. 108 (2016) 354–363, https://doi.org/10.1016/j.matdes.2016.06.112.
[10] F. Clabau, X. Rocquefelte, S. Jobic, P. Deniard, M. Whangbo, A. Garcia, J. Rouxel, Mechanism of phosphorescence appropriate for the long-lasting phosphors Eu^{2+}-doped $SrAl_2O_4$ with codopants Dy^{3+} and B^{3+}, Chem. Mater. 17 (2005) 3904–3912.
[11] H. Chander, D. Haranath, V. Shanker, P. Sharma, Synthesis of nanocrystals of long persisting phosphor by modified combustion technique, J. Cryst. Growth 271 (2004) 307–312, https://doi.org/10.1016/j.jcrysgro.2004.07.026.
[12] R.E. Rojas-Hernandez, F. Rubio-Marcos, A. Serrano, A. Del Campo, J.F. Fernandez, Precise tuning of the nanostructured surface leading to the luminescence enhancement in SrAl2O4 based core/shell structure, Sci. Rep. 7 (2017), 462. https://doi.org/10.1038/s41598-017-00541-w.
[13] Z. Pan, Y.-Y. Lu, F. Liu, Sunlight-activated long-persistent luminescence in the near-infrared from Cr3+-doped zinc gallogermanates, Nat. Mater. 11 (2011) 58–63, https://doi.org/10.1038/nmat3173.
[14] R. Chen, Y. Wang, Y. Hu, Z. Hu, C. Liu, Modification on luminescent properties of SrAl2O4:Eu2+, Dy3+ phosphor by Yb3+ ions doping, J. Lumin. 128 (2008) 1180–1184, https://doi.org/10.1016/j.jlumin.2007.11.094.
[15] A.K. Choubey, N. Brahme, D.P. Bisen, Synthesis of SrAl2O4:Eu phosphor by combustion method and its possible applications for mechanoluminescence dosimetry, Indian J. Pure Appl. Phys. 50 (2012) 851–854, https://doi.org/10.1088/1742-6596/187/1/012017.
[16] H. Terraschke, M. Suta, M. Adlung, S. Mammadova, N. Musayeva, R. Jabbarov, M. Nazarov, C. Wickleder, SrAl2O4:Eu2+(,Dy3+) nanosized particles: synthesis and interpretation of temperature-dependent optical properties Huayna, J. Spectrosc. 2015 (2015), https://doi.org/10.1016/j.jlumin.2007.11.015 (12 pp).
[17] Y. Wu, L. Wang, Y. Qing, N. Yan, C. Tian, Y. Huang, A green route to prepare fluorescent and absorbent nano-hybrid hydrogel for water detection, Sci. Rep. 7 (2017), 4380. https://doi.org/10.1038/s41598-017-04542-7.
[18] R.E. Rojas-Hernandez, M.a. Rodriguez, J.F. Fernandez, Role of the oxidizing agent to complete the synthesis of strontium aluminate based phosphors by the combustion method, RSC Adv. 5 (2015) 3104–3112, https://doi.org/10.1039/C4RA10460A.
[19] M.P. Anesh, S.K.H. Gulrez, A. Anis, H. Shaikh, M.E.A. Mohsin, S.M. Al-Zahrani, Developments in Eu+2-doped strontium aluminate and polymer/strontium aluminate composite, Adv. Polym. Technol. 33 (2014) 8–11, https://doi.org/10.1002/adv.21436.
[20] D. Dutczak, T. Jüstel, C. Ronda, A. Meijerink, Eu^{2+} luminescence in strontium aluminates, Phys. Chem. Chem. Phys. 17 (2015) 15236–15249, https://doi.org/10.1039/c5cp01095k.
[21] A.L. Yerokhin, X. Nie, A. Leyland, A. Matthews, S.J. Dowey, Plasma electrolysis for surface engineering, Surf. Coat. Technol. 122 (1999) 73–93, https://doi.org/10.1016/S0257-8972(99)00441-7.
[22] L.R. Krishna, A.S. Purnima, G. Sundararajan, A Comparative Study of Tribological Behavior of Microarc Oxidation and Hard-anodized Coatings, 261, 2006 1095–1101, https://doi.org/10.1016/j.wear.2006.02.002.
[23] A.L. Yerokhin, V.V. Lyubimov, R.V. Ashitkov, Phase formation in ceramic coatings during plasma electrolytic oxidation of aluminium alloys, Ceram. Int. 24 (1998) 1–6, https://doi.org/10.1016/S0272-8842(96)00067-3.
[24] V. Dehnavi, X.Y. Liu, B.L. Luan, D.W. Shoesmith, S. Rohani, Phase transformation in plasma electrolytic oxidation coatings on 6061 aluminum alloy, Surf. Coat. Technol. 251 (2014) 106–114, https://doi.org/10.1016/j.surfcoat.2014.04.010.
[25] R.H.U. Khan, A. Yerokhin, X. Li, H. Dong, A. Matthews, Surface characterisation of DC plasma electrolytic oxidation treated 6082 aluminium alloy: effect of current density and electrolyte concentration, Surf. Coat. Technol. 205 (2010) 1679–1688, https://doi.org/10.1016/j.surfcoat.2010.04.052.
[26] M. Mohedano, M. Serdechnova, M. Starykevich, S. Karpushenkov, A.C. Bouali, M.G.S. Ferreira, M.L. Zheludkevich, Active protective PEO coatings on AA2024: role of voltage on in-situ LDH growth, Mater. Des. 120 (2017) 36–46, https://doi.org/10.1016/j.matdes.2017.01.097.
[27] U. Malayoglu, K.C. Tekin, U. Malayoglu, S. Shrestha, An investigation into the mechanical and tribological properties of plasma electrolytic oxidation and hard-anodized coatings on 6082 aluminum alloy, Mater. Sci. Eng. A 528 (2011) 7451–7460, https://doi.org/10.1016/j.msea.2011.06.032.
[28] Z. Yao, Q. Xia, P. Ju, J. Wang, P. Su, D. Li, Z. Jiang, Investigation of absorptance and emissivity of thermal control coatings on Mg–Li alloys and OES analysis during PEO process, Sci. Rep. 6 (2016), 29563. https://doi.org/10.1038/srep29563.
[29] K. Du, X. Guo, Q. Guo, Y. Wang, F. Wang, Y. Tian, Effect of PEO coating microstructure on corrosion of Al 2024, J. Electrochem. Soc. 159 (2012) C597–C606, https://doi.org/10.1149/2.005301jes.
[30] M.P. Kamil, M. Kaseem, Y.G. Ko, Soft plasma electrolysis with complex ions for optimizing electrochemical performance, Sci. Rep. 7 (2017), 44458. https://doi.org/10.1038/srep44458.
[31] X. Lu, M. Mohedano, C. Blawert, E. Matykina, R. Arrabal, K.U. Kainer, M.L. Zheludkevich, Plasma electrolytic oxidation coatings with particle additions – a review, Surf. Coat. Technol. 307 (2016) 1165–1182, https://doi.org/10.1016/j.surfcoat.2016.08.055.
[32] K. Smits, D. Millers, A. Zolotarjovs, R. Drunka, M. Vanks, Luminescence of Eu ion in alumina prepared by plasma electrolytic oxidation, Appl. Surf. Sci. 337 (2015) 166–171, https://doi.org/10.1016/j.apsusc.2015.02.085.
[33] L. Grigorjeva, D. Millers, K. Smits, A. Zolotarjovs, Gas sensitive luminescence of ZnO coatings obtained by plazma electrolytic oxidation, Sensors Actuators A Phys. 234 (2015), https://doi.org/10.1016/j.sna.2015.09.018.
[34] S. Stojadinović, R. Vasilić, Formation and photoluminescence of Eu3+ doped zirconia coatings formed by plasma electrolytic oxidation, J. Lumin. 176 (2016) 25–31, https://doi.org/10.1016/j.jlumin.2016.03.012.
[35] A. Zolotarjovs, K. Smits, A. Krumina, D. Millers, L. Grigorjeva, Luminescent PEO coatings on aluminum, ECS J. Solid State Sci. Technol. 5 (2016) R150–R153, https://doi.org/10.1149/2.0401609jss.
[36] B. Li, M. Cao, J. Liu, Domain structure and enhanced electrical properties in sodium bismuth titanate ceramics sintered from crystals with different morphologies, J. Am. Ceram. Soc. 99 (2016) 2316–2326, https://doi.org/10.1111/jace.14211.
[37] M. Cao, X. Wang, W. Cao, X. Fang, B. Wen, J. Yuan, Thermally driven transport and relaxation switching self-powered electromagnetic energy conversion, Small 14 (2018), 1800987. https://doi.org/10.1002/smll.201800987.
[38] M. Cao, C. Han, X. Wang, M. Zhang, Y. Zhang, J. Shu, H. Yang, X. Fang, J. Yuan, Graphene nanohybrid: excellent electromagnetic properties for electromagnetic wave absorbing and shielding, J. Mater. Chem. C 6 (2018) 4586–4602, https://doi.org/10.1039/c7tc05869a.

[39] R.U. Din, V.C. Gudla, M.S. Jellesen, R. Ambat, Accelerated growth of oxide film on aluminium alloys under steam: part I: effects of alloy chemistry and steam vapour pressure on microstructure, Surf. Coat. Technol. 276 (2015) 77–88, https://doi.org/10.1016/j.surfcoat.2015.06.059.
[40] R.U. Din, V.C. Gudla, M.S. Jellesen, R. Ambat, Microstructure and corrosion performance of steam-based conversion coatings produced in the presence of TiO2particles on aluminium alloys, Surf. Coat. Technol. 296 (2016) 1–12, https://doi.org/10.1016/j.surfcoat.2016.03.093.
[41] T. Katsumata, K. Sasajima, T. Nabae, S. Komuro, T. Morikawa, Characteristics of strontium aluminate crystals used for long-duration phosphors, J. Am. Ceram. Soc. 81 (2005) 413–416, https://doi.org/10.1111/j.1151-2916.1998.tb02349.x.
[42] M. Nazarov, M.G. Brik, D. Spassky, B. Tsukerblat, Crystal field splitting of 5d states and luminescence mechanism in SrAl2O4:Eu2+phosphor, J. Lumin. 182 (2017) 79–86, https://doi.org/10.1016/j.jlumin.2016.10.015.
[43] Z. Li, K. Huang, Blue luminescence in porous anodic alumina films, J. Phys. Condens. Matter 19 (2007), 216203. https://doi.org/10.1088/0953-8984/19/21/216203.
[44] Y. Li, G.H. Li, G.W. Meng, L.D. Zhang, F. Phillipp, Photoluminescence and optical absorption caused by the F + centres in anodic alumina membranes, J. Phys. Condens. Matter 13 (2001) 2691–2699, https://doi.org/10.1088/0953-8984/13/11/323.
[45] T. Aitasalo, J. Hölsä, H. Jungner, J.C. Krupa, M. Lastusaari, J. Legendziewicz, J. Niittykoski, Effect of temperature on the luminescence processes of SrAl2O4:Eu2+, Radiat. Meas. 38 (2004) 727–730, https://doi.org/10.1016/j.radmeas.2004.01.031.
[46] V. Liepina, D. Millers, K. Smits, A. Zolotarjovs, X-ray excited luminescence of SrAl2O4:Eu,Dy at low temperatures, J. Phys. Chem. Solids (2018), https://doi.org/10.1016/j.jpcs.2017.12.040.
[47] M. Ayvacikli, A. Ege, N. Can, Radioluminescence of SrAl2O4:Ln3+(Ln = Eu, Sm, Dy) phosphor ceramic, Opt. Mater. (Amst) 34 (2011) 138–142, https://doi.org/10.1016/j.optmat.2011.07.023.
[48] A.N. Yerpude, S.J. Dhoble, Luminescence in trivalent rare earth activated Sr4Al 2O7 phosphor, Optik (Stuttg) 124 (2013) 3567–3570, https://doi.org/10.1016/j.ijleo.2012.11.064.
[49] W.M. Yen, S. Shionoya, H. Yamamoto, Phosphor Handbook, 2nd ed. CRC Press, 2006, https://doi.org/10.1109/MEI.2004.1342445.
[50] L. Xingdong, M. Zhong, R. Wang, Roles of Eu2+, Dy3+ions in persistent luminescence of strontium aluminates phosphors, J. Wuhan Univ. Technol. Mater. Sci. Ed. 23 (2008) 652–657, https://doi.org/10.1007/s11595-007-5652-7.
[51] P. Dorenbos, Mechanism of persistent luminescence in Eu2+ and Dy3+ codoped aluminate and silicate compounds, J. Electrochem. Soc. 152 (2005) 107–110, https://doi.org/10.1149/1.1926652.
[52] R. Chen, V. Pagonis, Thermally and Optically Stimulated Luminescence: A Simulation Approach, John Wiley & Sons, Ltd, 2011, https://doi.org/10.1002/9781119993766.
[53] R. Chen, Apparent stretched-exponential luminescence decay in crystalline solids, J. Lumin. 102–103 (2003) 510–518, https://doi.org/10.1016/S0022-2313(02)00601-4.
[54] M.N. Berberan-Santos, E.N. Bodunov, B. Valeur, Mathematical functions for the analysis of luminescence decays with underlying distributions 1. Kohlrausch decay function (stretched exponential), Chem. Phys. 315 (2005) 171–182, https://doi.org/10.1016/j.chemphys.2005.04.006.
[55] G. Barati Darband, M. Aliofkhazraei, P. Hamghalam, N. Valizade, Plasma electrolytic oxidation of magnesium and its alloys: mechanism, properties and applications, J. Magnes. Alloy. 5 (2017) 74–132, https://doi.org/10.1016/j.jma.2017.02.004.
[56] L.O. Snizhko, A.L. Yerokhin, N.L. Gurevina, V.A. Patalakha, A. Matthews, Excessive oxygen evolution during plasma electrolytic oxidation of aluminium, Thin Solid Films 516 (2007) 460–464, https://doi.org/10.1016/j.tsf.2007.06.158.
[57] L.O. Snizhko, A.L. Yerokhin, A. Pilkington, N.L. Gurevina, D.O. Misnyankin, A. Leyland, A. Matthews, Anodic processes in plasma electrolytic oxidation of aluminium in alkaline solutions, Electrochim. Acta 49 (2004) 2085–2095, https://doi.org/10.1016/j.electacta.2003.11.027.
[58] L.A. Snezhko, A.L. Erokhin, O.A. Kalinichenko, D.A. Misnyankin, Hydrogen release on the anode in the course of plasma electrolytic oxidation of aluminum, Mater. Sci. 52 (2016) 421–430, https://doi.org/10.1007/s11003-016-9974-5.
[59] C. Chang, Z. Yuan, D. Mao, Eu2+activated long persistent strontium aluminate nano scaled phosphor prepared by precipitation method, J. Alloys Compd. 415 (2006) 220–224, https://doi.org/10.1016/j.jallcom.2005.04.219.
[60] M. Ayvacikli, Z. Kotan, E. Ekdal, Y. Karabulut, A. Canimoglu, J. Garcia Guinea, A. Khatab, M. Henini, N. Can, Solid state synthesis of SrAl2O4:Mn2+ co-doped with Nd3+ phosphor and its optical properties, J. Lumin. 144 (2013) 128–132, https://doi.org/10.1016/j.jlumin.2013.06.040.
[61] S. Do Han, K.C. Singh, T.Y. Cho, H.S. Lee, D. Jakhar, J.P. Hulme, C.H. Han, J.D. Kim, I.S. Chun, J. Gwak, Preparation and characterization of long persistence strontium aluminate phosphor, J. Lumin. 128 (2008) 301–305, https://doi.org/10.1016/j.jlumin.2007.07.017.

Institute of Solid State Physics, University of Latvia as the Center of Excellence has received funding from the European Union's Horizon 2020 Framework Programme H2020-WIDESPREAD-01-2016-2017-TeamingPhase2 under grant agreement No. 739508, project CAMART²